

# LHRH Receptor Monoclonal Antibody 4F3B10 Induces Apoptosis of HeLa Cells

Xin Deng<sup>1#</sup>, Peipei Zhang<sup>2#</sup>, Guoli Zhang<sup>3,\*</sup>

<sup>1</sup>Central Laboratory, The Fourth Affiliated Hospital of China Medical University, Shenyang 110122, China

<sup>2</sup>Beijing TransGen Biotech Company, Beijing, 100192, China

<sup>3</sup>Military Veterinary Institute of Military Medical Science Academy, 130122, China

\*Corresponding author: Guoli Zhang, E-mail: zhangguoli2001@126.com

#These authors contributed equally to this work.

## Abstract

**Background:** Cellular receptors that overexpressed in the tumor tissues are effective targets for the development of specific targeting agents for cancer cells. These drugs have high specificity for target organs and reduced side effects in patients. Overexpression of luteinizing hormone releasing hormone receptor (LHRHR) has been reported in some solid tumors. Here, we investigated the effect and mechanism of the LHRHR monoclonal antibody 4F3B10 on HeLa cells.

**Methods:** Gene expression profiles were utilized to screen the differentially expressed genes in HeLa cells with the effects of antagonist 4F3B10 and analyze the relation among the differentially expressed genes by bioinformatics analysis. CCK-8 assays and flow cytometry were used for detecting the proliferation and apoptosis of HeLa cells induced by 4F3B10.

**Results:** CCK-8 assays and flow cytometry showed that 4F3B10 inhibited proliferation and induced apoptosis of HeLa cells in a dose-dependent manner. Furthermore, 4F3B10 inhibited the cell cycle progression of HeLa cells at G1 phase. Microarray analysis identified 2329 differentially expressed genes between HeLa cells treated with 4F3B10 and untreated cells. Apoptotic genes encoding Caspase6, Caspase8, Caspase10, CFLAR, FASLG, IRAK2, PPP3CB, PPP3CC, PPKAR2A and TNFRSF10D were upregulated in HeLa cells treated with 4F3B10. RTqPCR was performed to validate the microarray findings.

**Conclusions:** Here we demonstrate the anti-cancer effects of the LHRHR 4F3B10 monoclonal antibody in HeLa cancer cells, including significant effects on cell cycle progression, proliferation and induction of apoptosis. Our results identified several key differentially expressed apoptotic genes and support further study of the molecular mechanism of LHRHR.

**Key words:** Luteinizing hormone releasing hormone receptor (LHRHR); 4F3B10 (LHRHR monoclonal antibody); HeLa cells

## Background

Cancer-targeting delivery is usually achieved by adding a ligand moiety to a drug delivery system to help direct specific binding to cancer cells, such as via cellular receptors [1]. Over the past decades, research efforts have developed several selective anticancer drugs with demonstrated less cytotoxic side effects [2-7].

Luteinizing hormone releasing hormone (LHRH), also known as gonadotropin releasing hormone 1, is a peptide hormone that is responsible for the release of follicle-stimulating hormone and luteinizing hormone from the anterior pituitary. The elevated LHRH receptor (LHRHR) levels in malignant cancer tissues make these cancers highly sensitive to the mitogenic and anti-apoptotic activity of LHRH [6,8]. Based on this knowledge, LHRH has been used as a targeting moiety in drug delivery systems to enhance drug uptake to malignant cancer cells and reduce the toxicity in normal cells.

Microarrays have been widely used due to their extensive detection range and accuracy [9-15]. Researchers have evaluated many differentiation-inducing agents that affect the proliferation and differentiation of tumor cells or may induce apoptotic cell death in cancer cells [16,17].

Here, we developed a novel monoclonal antibody (4F3B10) targeting LHRHR and investigated the effect and mechanism of the LHRHR monoclonal antibody 4F3B10 on HeLa cells.

## Methods

### Cell culture

HeLa cells (human carcinoma cervical cells) were purchased from the Cell Bank of Chinese Academy of Science (Shanghai, China). HeLa cells were cultivated in T25 culture flasks in Roswell Park Memorial Institute (RPMI) 1640 (Gibco, USA), supplemented with 10% fetal bovine serum (FBS) (Hyclone, Lanzhou, China) and 1% penicillin/streptomycin (Cellgro, Mediatech Inc., VA, USA) in a humidified 5% CO<sub>2</sub> atmosphere at 37°C. Cells were passaged approximately at 80% confluence and the media was replaced every 2 or 3 days. The monoclonal antibodies against LHRHR (4F3B10) were established by Professor Guoli Zhang at the Institute of Military Veterinary of Academy of Military Medical Sciences using routine hybridoma techniques.

### CCK-8 assay

HeLa cells were seeded into 96-well tissue culture plates at a density of  $1 \times 10^5$  cells per well and stimulated with 4F3B10 at various concentrations of 0.067, 0.134, 0.267, 0.536 and 0.804  $\mu\text{mol/L}$  for 48 h. Three replicate wells were used for every sample. Next, 10  $\mu\text{l}$  of CCK8 (DOJINDO) was added to each well. After 1 h, the absorbance of samples was read using a 96-well plate reader (ELISA Reader) at a wavelength of 450 nm. Each data point was determined eight times prior to analysis. Statistical analysis of the cell proliferation assay was performed with the Graphpad Prime5.

### Flow cytometric analysis of cell cycle

The DNA contents during cell cycle were evaluated with flow cytometry. In brief,  $5 \times 10^6$  HeLa cells were treated with 4F3B10 at concentrations of 0.067 or 0.267  $\mu\text{mol/L}$ . After 48 h, cells were harvested, washed and resuspended in 1 ml of 70% cold ethanol in PBS, followed by incubation for 1 h at 4°C. Cells were washed twice in PBS. Next, 500  $\mu\text{l}$  of propidium iodide (PI; SIGMA-ALDRICH®, Steinem, Germany) staining buffer (50  $\mu\text{g/ml}$  PI, 10  $\mu\text{g/ml}$  RNase in PBS) was added and cells were incubated for 1 h at room temperature in the dark. Samples were then evaluated by a flow cytometer. Analysis was performed by FACSCalibur using 488 nm excitation and a 610 nm filter for PI detection.

### Apoptosis assay

HeLa cells ( $1 \times 10^6$  cells/ml) were treated with 4F3B10 (concentrations of 0.067 or 0.267  $\mu\text{mol/L}$ ) for inducing apoptosis and cultured in 5%  $\text{CO}_2$  incubator for 48 h at 37°C. Untreated cells were used as a negative control. Cells were then washed twice with PBS and resuspended in  $1 \times$  binding buffer at a concentration of  $1 \times 10^6$  cells/ml. Next, 500  $\mu\text{l}$  of the cell suspension was mixed with 5  $\mu\text{l}$  of AnnexinV-FITC (BD) and 5  $\mu\text{l}$  of PI (BD). The tubes were incubated at room temperature for exactly 10 min and protected from light. Cells were analyzed on a FACSCalibur using 488 nm excitation and a 525 nm bandpass filter for fluorescent detection.

### Transcriptome analyses

After reaching confluence, cells for force measurement were seeded directly onto 35-mm Petri dishes for 24 h. Before experiments, the subconfluent cells (at about 80% confluence) were rinsed 10 times with phosphate buffer saline (PBS; 137 mM NaCl, 2 mM KCl, 8 mM  $\text{Na}_2\text{HPO}_4$ , 1.5 mM  $\text{KH}_2\text{PO}_4$ , and pH 7.4). An 8 ml sample of planktonic culture was withdrawn and the cells were pelleted by centrifugation at  $5000 \times g$  for 10 min at 4°C. To collect biofilm cells, pieces of cotton towel were harvested from the fermentation broth and rinsed twice with ice-cold PBS buffer in the anaerobic system within one minute to remove contaminating planktonic cells. The cotton towel was submerged in 8 ml ice-cold PBS buffer and immediately vortexed vigorously for 40 s to disperse the adsorbed cells. The cotton towel was removed and the resulting suspension was centrifuged at  $8000 \times g$  for 6 min at 4°C to pellet the biofilm cells. All the cells were frozen immediately using liquid nitrogen and stored at  $-80^\circ\text{C}$  prior to RNA extraction.

### Total RNA extraction, purification, and labeling

Total RNA was extracted from HeLa cells using TRIZOL reagent following the manufacturer's instructions. RIN (RNA integrity number) was checked by an Agilent Bioanalyzer 2100. Qualified total RNA was further purified by the RNeasy mini kit (Cat#74106, QIAGEN, GmbH, Germany) and RNase-Free DNase Set (Cat#79254, QIAGEN). Total RNA was amplified and labeled by the Low Input Quick Amp Labeling Kit, One-Color (Cat#5190-2305, Agilent Technologies, Santa Clara, CA, US), following the manufacturer's instructions. Labeled cRNAs were purified by the RNeasy mini kit (Cat#74106, QIAGEN).

### Microarray hybridization, washing, and scanning

Single color microarray assays were performed by Shanghai Biochip Co. Ltd. according to standard protocols provided by Agilent Technologies. In brief, each slide was hybridized with 600 ng Cy3-labeled cRNA using the Gene Expression Hybridization Kit in a hybridization oven. After 17 h, slides were washed in staining dishes with the Gene Expression Wash Buffer Kit. Slides were scanned by the Agilent Microarray Scanner with default settings (dye channel: green, scan resolution = 5 m, PMT 100%, 10%, 16 bit). Data were extracted with Feature Extraction software 10.7. Raw data were normalized by Quantile algorithm, Gene Spring Software 11.0.

### Microarray data analysis

Two biological replicates were performed for microarray data analysis. One sample was withdrawn from each replicate at each time point. The sample sets of the two biological replicates were hybridized to the microarray separately. Variation between the two sets of data was small. Quantitative RT-PCR was used to confirm the microarray results of several selected genes (Table 1). The results of the RT-PCR and the microarray patterns showed good agreement: most genes showed quantitative agreement (a similar fold change in expression levels) and all the genes exhibited expression pattern agreement (upregulation or downregulation), suggesting a good quality of the microarray data. Gene expression with a  $\log_2$  (ratio)  $\geq 1.0$  was considered upregulated expression, and gene expression with a  $\log_2$  (ratio)  $\leq -1.0$  was considered downregulated expression.

Table 1 Names and sequences of primers

Gene Name	Primer sequence (5'-3')	PCR (bp) product	GenBank
ECI2	F: GCATCTGACAGGGCAACAT R: TGGCTGGGCTCATTATCTT	100	NM_206836.3
PRKAR2A	F: GGAGGAGGACGAGGACTTG R: GGATGAATCACCTTGGAT	123	NM_004157.2
CDC42	F: GGCTGTCAAGTATGTGG R: GCAAAGAAGGGAAGGA	152	NM_044472.2
CASP6	F: TTAAGTGGCTTGTTCAAAG R: CAGCGTGTAACGGAGG	186	NM_001226.3
GNAQ	F: GGAGAGAGTGGCAAGAGTACG R: TTGTGCATGAGCCTTATTGTGC	192	NM_002072.4

### Enrichment analysis of the GO and pathway analysis

The functional categorizations of significantly changed genes were annotated by reference to the Gene Ontology (GO) (<http://www.geneontology.org/>) and NCBI GENE databases (<http://www.ncbi.nlm.nih.gov/gene>). The physiological function of these genes was identified according to the Kyoto Encyclopedia of Genes and Genomes (KEGG) (<http://www.genome.jp/kegg/kegg2.html>). Finally, the differentially expressed genes were classified according to their function.

The Shbioship (SBC) online analysis system provided by Bohao Company was used for analyses (<http://SAS.ebioservice.com>). The fold value (the difference in fold) represents the degree of differential expression between the untreated and 4F3B10-treated HeLa cells. The standard for judging differential expression was as follows: the differentially expressed genes screened from the 4F3B10 group were used as valid genes. Compared to the control group, a gene with a fold change  $<0.5$  was considered as a downregulated gene, while a gene with a fold change  $> 2.0$  was considered as an upregulated gene.

### Real-time quantitative reverse-transcription PCR analysis (RTqPCR)

The microarray gene expression profiles were confirmed by quantitative real-time PCR (qPCR). The gene expression levels were determined by real-time PCR analysis. RNA was isolated and purified as described above. The concentration and purity were assessed by a spectrophotometer (SmartSpec Plus, Bio-Rad Laboratories, Inc., Hercules, CA, USA) based on the OD260/OD280 ratio. The PrimeScript<sup>TM</sup> RT reagent kit with gDNA Eraser (Perfect Real Time) (Cat. #RR047A, TAKARA) was used for reverse transcription of the RNA. The 10  $\mu$ l genomic DNA elimination reaction consisted of 2  $\mu$ l 5  $\times$  gDNA Eraser Buffer, 1  $\mu$ l Eraser Buffer, 1  $\mu$ g total RNA. The reaction mix was incubated for 2 min at 42°C and held at 4°C. The reverse-transcription reaction consisted of 10  $\mu$ l of the genomic DNA elimination reaction, 4.0  $\mu$ l 5 $\times$  PrimeScript Buffer 2 (for real time), 1  $\mu$ l PrimeScript RT Enzyme MixI, 1  $\mu$ l RT Primer Mix, and 4  $\mu$ l RNase Free dH<sub>2</sub>O. The reaction mix was incubated for 15 min at 37°C, for 5 s at 85°C and held at 4°C. The 20  $\mu$ l PCR reaction consisted of 10  $\mu$ l SYBR primer Ex Taq II (Tli RNaseH Plus) (2 $\times$ ), 0.8  $\mu$ l PCR forward primer (10  $\mu$ M), 0.8  $\mu$ l reverse primer (10  $\mu$ M), ROX reference dye (50 $\times$ ), 2  $\mu$ l template and 6  $\mu$ l dH<sub>2</sub>O. The reactions were performed in triplicate with an AB

7500 System at a total volume of 20  $\mu$ l. The following PCR program was used: 10 min at 95°C, 40 cycles of 30 s at 95°C and 1 min at 60°C. The Beta2-M gene was amplified in parallel with the target genes and used as an internal control. All samples were amplified in triplicate and the mean value was determined. The change-fold was the mean  $\pm$  SD of the two biological replicates.

Expression levels were determined using the relative cycle threshold (CT) method as described by the manufacturer (Stratagene). Each gene was calculated by evaluating the expression of  $2^{-\Delta\Delta CT}$ , where  $\Delta\Delta CT$  is the result of the following:  $[CT_{\text{gene}} - CT_{\beta\text{-actin}}] (\text{stress}) - [CT_{\text{gene}} - CT_{\beta\text{-actin}}] (\text{control})$ .

### Statistical analysis

Differences between the two groups were determined by Student's t test for samples by equal variance with SPSS 13.0 software (SPSS, Chicago, IL, USA). The data are expressed as the means  $\pm$  standard deviations of three independent experiments. Values of  $p < 0.05$  were considered statistically significant.

## Results

### Anti-proliferative and inhibitory effects of 4F3B10

We first examined the anti-proliferative effects of 4F3B10 on HeLa cells using the CCK-8 assay. The results of one representative experiment are shown in Figure 1. The results showed that 4F3B10 inhibited the proliferation of HeLa cells in a concentration-dependent manner. The most significant inhibitory effects of 4F3B10 in HeLa cells after 48 h were observed at concentrations of 0.267  $\mu$ mol/L, 0.536  $\mu$ mol/L and 0.804  $\mu$ mol/L. The effective dose that inhibited 50% proliferation (IC<sub>50</sub>) of cells after 48 h treatment was approximately 60.16  $\mu$ g/mL (Fig. 1).

### Cell cycle analysis

We next evaluated the effect of 4F3B10 on the cell cycle distribution of HeLa cells (Fig. 2). In control untreated HeLa cells, 58.19% of cells accumulated in G<sub>1</sub> phase and 12.72% of cells were in S phase (Fig. 2A). In comparison, in HeLa cells treated with 10  $\mu$ g/ml or 40  $\mu$ g/ml 4F3B10, we observed 66.6% and 74.04% of cells in G<sub>1</sub> phase and a significant decrease of S phase cells to 7.74% and 5.74%, respectively (Fig. 2B and 2C).



## Apoptosis

We examined the effects of 4F3B10 on inducing apoptosis in HeLa cells using AnnexinV-FITC staining and flow cytometry. The results showed that the percentages of apoptotic cells were significantly increased upon treatment with 10  $\mu\text{g/ml}$  and 40  $\mu\text{g/ml}$  4F3B10 (Fig. 3).

## Transcriptome analyses

To study the effect of 4F3B10 on HeLa cells from the transcriptome aspect, we used microarray technology to screen differentially expressed genes. The microarray results revealed a total of 2329 differentially expressed genes that showed a change in gene expression by at least two-fold in 4F3B10-treated HeLa cells compared with control cells ( $p < 0.05$ ).

To investigate the biological functions of these differentially expressed genes, we performed Gene Ontology (GO) category analysis. The differentially expressed genes were assigned to the categories of biological process, cellular component, and molecular function. GO annotation was further performed for the 2329 differentially expressed genes in the categories of biological process, molecular function and cellular component. The highly represented GO terms were cellular process, biological regulation, metabolic process and response to stimulus for biological processes; binding, catalytic activity and molecular transducer activity for molecular function; and cell parts, cells and organelles for the cellular component. We used the GO function to analyze the differential gene classification and the results show that there were 71.9% differentially expressed genes in biological pathways involved in hormone stimulation, growth regulators, regeneration, signal transduction, apoptosis gene product activation, and chromatin modification; 20.3% differentially expressed genes in cellular component involved in basement membrane, laminin, enzyme complexes, and nucleolus; and 7.8% differentially expressed genes in molecular function involved in growth factor binding, ion binding, and enzyme activity between 4F3B10-treated and control HeLa cells (Fig. 4).

Pathway enrichment analysis indicated that some differentially expressed genes were mainly involved in a total of 17 pathways (values of  $p < 0.05$ ), including adhesion and diapedesis of granulocytes, the FAS signaling pathway (CD95) and apoptosis (Fig. 5). Figure 6 shows a general schematic of the FAS signaling pathway



(CD95) and six genes in this pathway (indicated with the red outline) were differentially expressed between 4F3B10-treated and control HeLa cells. Figure 7 shows a general schematic of the apoptosis signaling pathway and nine genes in this pathway (indicated with the red outline) were differentially expressed between 4F3B10-treated and control HeLa cells. These genes (indicated with the red outline) are identified in the microarray results.

To validate the consistency of microarray analysis results, we compared the gene expression levels of five randomly selected genes (ECI2, PRKAR2A, CASP6, GNAQ and CDC42 genes) between microarray and real-time PCR using specific primers (Table 1). We determined the mean value of expression of the selected genes in HeLa cells treated with 4F3B10 and control cells. Although in the 4F3B10-treated group, ECI2 mRNA levels ( $P=0.163$ ) showed no significant differences in expression compared with the control group, PRKAR2A mRNA ( $P = 0.043$ ), CDC42 mRNA ( $P = 0.002$ ), CASP6 mRNA ( $P = 0.011$ ) and GNAQ mRNA ( $P = 0.014$ ) showed significant differences in expression compared with the control group. The overall results showed that the qualitative changes in gene expression levels were consistent between these analyses and confirm the microarray results (Fig. 8 and 9).

Amplification of RNA may introduce bias into transcript abundance assays. However, we confirmed that the quality of the RNA complied with the requirements of the experiment (Table 2).

Table 2. Quality control information of RNA samples

No	Sample Name	Con. / ( $\mu\text{g}/\mu\text{l}$ )	Vol. / ( $\mu\text{l}$ )	Total/ ( $\mu\text{g}$ )	A260/ A280	2100 RIN	Result 28S/18S
1	The control	1.721	30	51.63	1.94	9.4	2.0
2	4F3B10-treated	1.876	30	56.28	1.94	9.8	2.0

## Discussion

Reports over recent years have shown that targeted cancer drugs exhibit significant effects on their corresponding cancers, with much fewer side effects than that of chemotherapy. Previous studies showed that the occurrence and development of some cancers have certain correlations with the expression of LHRHR [18]. LHRH, its analogues and recombinant toxin with LHRH as the target can inhibit the growth of

some cancer cells via LHRH receptor [19-21].

Aberrant cell proliferation, cell cycle and apoptosis pathways are essential to the development and occurrence of cancer [22,23]. Here we produced a monoclonal antibody against LHRHR, named 4F3B10. We detected morphological changes in HeLa cells treated with 4F3B10 using an inverted microscope (data not shown) and analyzed the effect of 4F3B10 on HeLa cell proliferation, cell cycle and apoptosis.

Our CCK-8 results showed that with increasing 4F3B10 concentration, the survival rate of HeLa cells decreased. At the concentration of 0.267  $\mu\text{mol/L}$  4F3B10, the survival rate decreased significantly. We also found that 4F3B10 treatment of HeLa cells caused an increase in  $G_1$  phase cells and decrease of S phase cells compared with untreated HeLa cells, indicating that 4F3B10 inhibited HeLa cell cycle progression. We also detected apoptosis of HeLa cells treated with 4F3B10 at 0.267  $\mu\text{mol/L}$ , but not at the lower concentration of 0.067  $\mu\text{mol/L}$ .

We next performed microarray analysis to identify differentially expressed genes in 4F3B10-treated cells and conducted bioinformatics analysis of the differentially expressed genes. Our results identified 1589 upregulated genes and 738 downregulated genes in HeLa cells treated with 4F3B10. These results indicate the effects of 4F3B10 on HeLa cells may involve complex biological processes and multiple genes. KEGG enrichment analysis showed that some of the differentially expressed genes in HeLa cells treated with 4F3B10 are involved in FAS (CD95) and apoptosis signaling pathways.

The FAS signaling pathway leading to apoptosis involves FAS (also called CD95) crosslinking with FAS ligand (FASL or CD95L), resulting in the formation of a death-inducing signaling complex (DISC) composed of CD95, the signal adaptor protein FADD, and procaspase-8 [10-13]. This association generates CASP8 and activates a cascade of caspases [14]. Lepple-Wienhues et al. showed that in addition to the role of CD95 in inducing cell death, stimulation of CD95 inhibits the influx of calcium normally induced by activation of the T-cell antigen receptor, in part by not affecting the release of calcium from intracellular stores. This block in calcium entry can be mimicked by stimulating T cells with acid sphingomyelinase metabolites of the plasma membrane lipid sphingomyelin, such as ceramide and sphingosine [15]. Chen et al. demonstrated that CD95 has a growth-promoting role during tumorigenesis and indicated that efforts to inhibit its activity should be considered during cancer therapy.

In conclusion, our findings demonstrating the anti-cancer effects of the 4F3B10

monoclonal antibody in HeLa cancer cells provide a basis for further study of the molecular mechanism of LHRHR. Our microarray analysis provided a substantial amount of information to help us determine the cellular changes induced by the 4F3B10 monoclonal antibody. KEGG analysis revealed multiple pathways affected by 4F3B10, including FAS signaling pathway and apoptosis. Our future studies will focus on several key proteins in LHRHR-related pathways to examine the effect of 4F3B10 on apoptosis. While our initial microarray analysis was focused on differentially expressed mRNA levels, we also identified a series of differentially expressed long non-coding RNAs. Research has shown that long non-coding RNAs are also involved in the occurrence and metastasis of cancer [24-27], and thus these factors should be examined in further studies.

### **Conclusions**

Here we demonstrate the anti-cancer effects of the LHRHR 4F3B10 monoclonal antibody in HeLa cancer cells, including significant effects on cell cycle progression, proliferation and induction of apoptosis.

### **Abbreviations**

CCK-8: Cell Counting Kit; PBS: phosphate buffer saline; PI: propidium iodide; RTqPCR: Real-time quantitative reverse-transcription PCR; GO: Gene Ontology; KEGG: Kyoto Encyclopedia of Genes and Genomes.

### **Declarations**

Not applicable

### **Ethics approval and consent to participate**

Consent for publication

### **Availability of data and material**

The data set supporting the results of this article is available in the NCBI Sequence Read Archive (<https://www.ncbi.nlm.nih.gov/geo/query/acc.cgi?acc=GSE95695>).

### **Competing interests**

The authors declare that they have no competing interests.

### **Funding**

The authors acknowledge the financial support of National Natural Science Function of China, 81370712 and 31172165.

### **Authors' contributions**

XD and PpZ designed and performed the research studies, analyzed the data, and wrote the manuscript. GLZ designed the study, provided overall guidance, and helped write the manuscript. All authors read and approved the final manuscript.

## References

1. Dharap S S, Wang Y, Chandna P, et al. Tumor-specific targeting of an anticancer drug delivery system by LHRH peptide. *Proc Nati Acad Sci USA*. 2005; 102:12962-7.
2. Sarnovsky R, Tendler T, Makowski M, et al. Initial characterization of an immunotoxin constructed from domains II and III of cholera exotoxin. *Cancer Immunol Immun Cii*, 2010;59: 737-46.
3. Kreitman RJ, Stetler-Stevenson M, Margulies I, et al. Phase II trial of recombinant immunotoxin RFB4(dsFv)-PE38 (BL22) in patients with hairy cell leukemia. *J Clin Oncol*. 2009; 27:2983-90.
4. Kreitman RJ. Recombinant Immunotoxins containing truncated bacterial toxins for the treatment of hematologic malignancies. *Biodrugs*. 2009;23:1-13.
5. Onda M, Beers R, Xiang L, Nagata S, Wang QC, Pastan I. An immunotoxin with greatly reduced immunogenicity by identification and removal of B cell epitopes. *Proc Nati Acad Sci USA*. 2008;105:11311-6.
6. Deng X, Klussmann S, Wu G M, Wu GM, Akkerman D, Zhu YQ, Liu Y, Chen H, Zhu P, Yu B, Zhang GL. Effect of LHRH-PE40 on target cells via LHRH receptors. *J Drug Target*. 2008;16:379-88.
7. Kreitman RJ, Squires DR, Stetler-Stevenson M, Noel P, FitzGerald DJ, Wilson WH, Pastan I. Phase I trial of recombinant immunotoxin RFB4(dsFv)-PE38 (BL22) in patients with B-cell malignancies. *J Clin Oncol*. 2005;23:6719-29.
8. Deng X, Zhang GL, Zhang Li, Feng Y, Li ZH, Wu GM, Yue YH, Cao Y, Zhu P. Developing a novel gene-delivery vector system using the recombinant fusion protein of *Pseudomonas* exotoxin A and hyperthermophilic archaeal histone HPhA. *PLoS One*. 2015 Nov 10;10(11): e0142558. doi: 10.1371/journal.pone.0142558.
9. Hueber AO. CD95: more than just a death factor? *Nat Cell Biol*. 2000; 2(2): E23-5.
10. Fouqué A, Deburé L, Legembre P. The CD95/CD95L signaling pathway: a role in carcinogenesis. *Biochim Biophys Acta*. 2014;1846:130-41.
11. Lepple-Wienhues A, Belka C, Laun T, Jekle A, Walter B, Wieland U, Welz M, Heil L, Kun J, Busch G, Weller M, Bamberg M, Gulbins E, Lang F. Stimulation of CD95 (Fas) blocks T lymphocyte calcium channels through sphingomyelinase and sphingolipids. *Proc Nat Acad Sci USA*. 1999;96:13795-800.
12. Rimbault M, Robin S, Vaysse A, Galibert F. RNA profiles of rat olfactory epithelia: Individual

and age related variations. *BMC Genom.* 2009;10:572.

13.Sammata N, Yu TT, Bose SC, McClintock TS. Mouse olfactory sensory neurons express 10,000 genes. *J Comp Neurol.* 2007;502:1138-56.

14.Nickell MD, Breheny P, Stromberg AJ, McClintock TS. Genomics of mature and immature olfactory sensory neurons. *J Comp Neurol.* 2012;520:2608-29.

15.Yazdanparast R, Moosavi M, Mahdavi M, Lotfi A. Guanosine 5'-triphosphate induces differentiation dependent apoptosis in human leukemia U937 and KG1 cells. *Acta Pharmacol Sin.* 2006;27:1175-84.

16.Sun SY, Hail N Jr, Lotan R. Apoptosis as a novel target for cancer chemoprevention. *J Natl Cancer Inst.* 2004;96:662-72.

17.Meyer C1, Sims AH, Morgan K, Harrison B, Muir M, Bai J, Faratian D, Millar RP, Langdon SP. Transcript and protein profiling identifies signaling, growth arrest, apoptosis, and NF-kB survival signatures following GNRH receptor activation *Endocr Relat Cancer.* 2013;20:123-36.

18.Maggi R, Cariboni AM, Marelli MM, Moretti RM, Andr  V, Marzagalli M, Limonta P. GnRH and GnRH receptors in the pathophysiology of the human female reproductive system. *Hum Reprod Update*, 2016;22: pii: dm059. doi: 10.1093/humupd/dm059. Epub 2015 Dec 29. Review.

19.Limonta P, Manea M. Gonadotropin-releasing hormone receptors as molecular therapeutic targets in prostate cancer: Current options and emerging strategies. *Cancer Treat Rev.* 2013;39:647-63.

20.Popovics P, Schally AV, Szalontay L, Block NL, Rick FC. Targeted cytotoxic analog of luteinizing hormone-releasing hormone (LHRH), AEZS-108 (AN-152), inhibits the growth of DU-145 human castration-resistant prostate cancer in vivo and in vitro through elevating p21 and ROS levels. *Oncotarget* 2014;5:4567-78.

21.Wang W, El-Deiry WS. Restoration of p53 to limit tumor growth. *Curr Opin Oncol.* 2008;20:90-6.

22.Fingerman IM, Briggs SD. p53-mediated transcriptional activation: from test tube to cell. *Cell.* 2004;117:690-1.

23.Fang TT, Sun XJ, Chen J, Zhao Y, Sun RX, Ren N, Liu BB. Long non-coding RNAs are differentially expressed in hepatocellular carcinoma cell lines with differing metastatic potential. *Asian Pac J Cancer Prev.* 2014;15:10513-24.

24.Yuan JH, Yang F, Wang F, Ma JZ, Guo YJ, Tao QF, Pan W, Wang TT, Zhou CC, Wang SB, Wang YZ, Yang Y, Yang N, Zhou WP, Yang GS, Sun SH. A long noncoding RNA activated by TGF- $\beta$  promotes the invasion-metastasis cascade in hepatocellular carcinoma. *Cancer Cell* 2014;25:666-81.

25.Yang C, Li X, Wang Y, Zhao L, Chen W. Long non-coding RNA UCA1 regulated cell cycle distribution via CREB through PI3-K dependent pathway in bladder carcinoma cells. *Gene* 2012;496:8-16.

26.Gao Y, Chen G, Zeng Y, Zeng J, Lin M, Liu X, Liu J. Invasion and metastasis-related long noncoding RNA expression profiles in hepatocellular carcinoma. *Tumour Biol.* 2015;36:7409-22.

27.He Y, Meng XM, Huang C, Wu BM, Zhang L, Lv XW, Li J. Long noncoding RNAs: Novel insights into hepatocellular carcinoma. *Cancer Lett.* 2014;344:20-7.

### Figure Legends

#### **Figure 1. The anti-proliferative effects of 4F3B10 on HeLa cells**

HeLa cells were treated with the indicated concentrations of 4F3B10 for 48 h. Cell proliferation was evaluated by CCK8 assays.  $^{**}p < 0.01$  compared with untreated cells.

#### **Figure 2. Effect of 4F3B10 treatment on cell cycle progression of HeLa cells**

Untreated HeLa cells (A) or HeLa cells treated with 4F3B10 at 0.067  $\mu\text{mol/L}$  (B) or 0.267  $\mu\text{mol/L}$  (C) for 48 h were analyzed by flow cytometry for evaluation of cell cycle distribution.

#### **Figure 3. Apoptosis of HeLa cells induced by 4F3B10**

Untreated HeLa cells (A) or HeLa cells treated with 4F3B10 at 0.067  $\mu\text{mol/L}$  (B) or 0.267  $\mu\text{mol/L}$  (C) for 48 h were analyzed by flow cytometry for evaluation of apoptosis rate. FL1-H: Annexin V-FITC; FL2-H: PI. Lower left quadrant, viable cells; lower right quadrant, necrotic cells; upper left quadrant, early apoptotic cells; upper right quadrant, nonviable late apoptotic cells.

#### **Figure 4. Gene ontology (GO) analysis of differentially expressed genes in HeLa cells treated with 4F3B10**

The 2329 differentially expressed genes in HeLa cells treated with 4F3B10 were subjected to GO analysis using the SBC (Shanghai Biotechnology Corporation) Analysis System. The results are summarized in a bar chart showing the number of genes associated with each GO term ( $p < 0.05$ ).

#### **Figure 5. KEGG pathway analysis of differentially expressed genes in HeLa cells treated with 4F3B10**

The 2329 differentially expressed genes were subjected to KEGG pathway analysis using the SBC Analysis System. The results are summarized in a bar chart showing the number of genes associated with each cellular pathway/process ( $p < 0.05$ ).

#### **Figure 6. Apoptosis signaling pathway**

A general schematic of the apoptosis signaling pathway and nine genes in this

pathway (indicated with the red outline) were differentially expressed between 4F3B10-treated and control HeLa cells.

**Figure 7. Quantitative real-time PCR confirmation of the microarray data**

Quantitative PCR was performed on five differentially expressed genes randomly selected from the microarray results. Each sample was measured in triplicate. Columns, mean of two treated samples in the microarray experiment; bars, SD. \* $p < 0.05$  compared to the control by the  $t$ -test.

**Figure 8. Protein Expression Detection**

Protein levens were performed on five differentially expressed Proteins, LYN, BTK, CASP8, FAS and  $\beta$ 2-M, randomly selected from the microarray results.

Figure 1

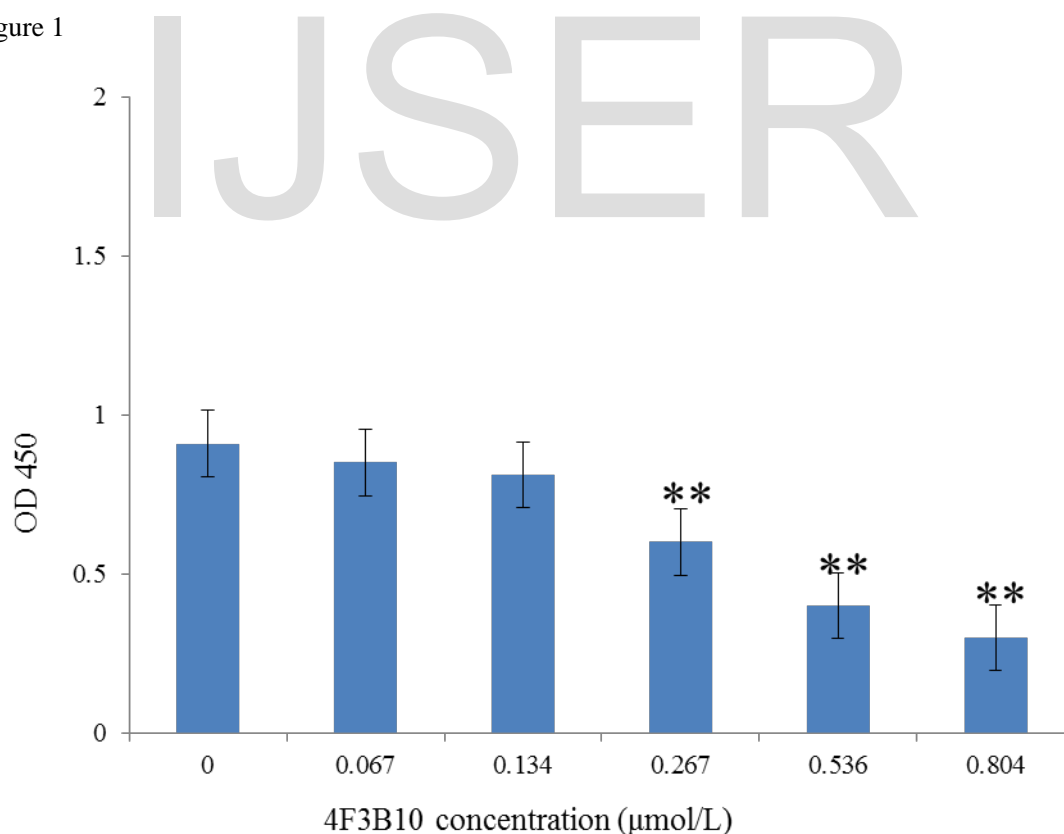




Figure 2

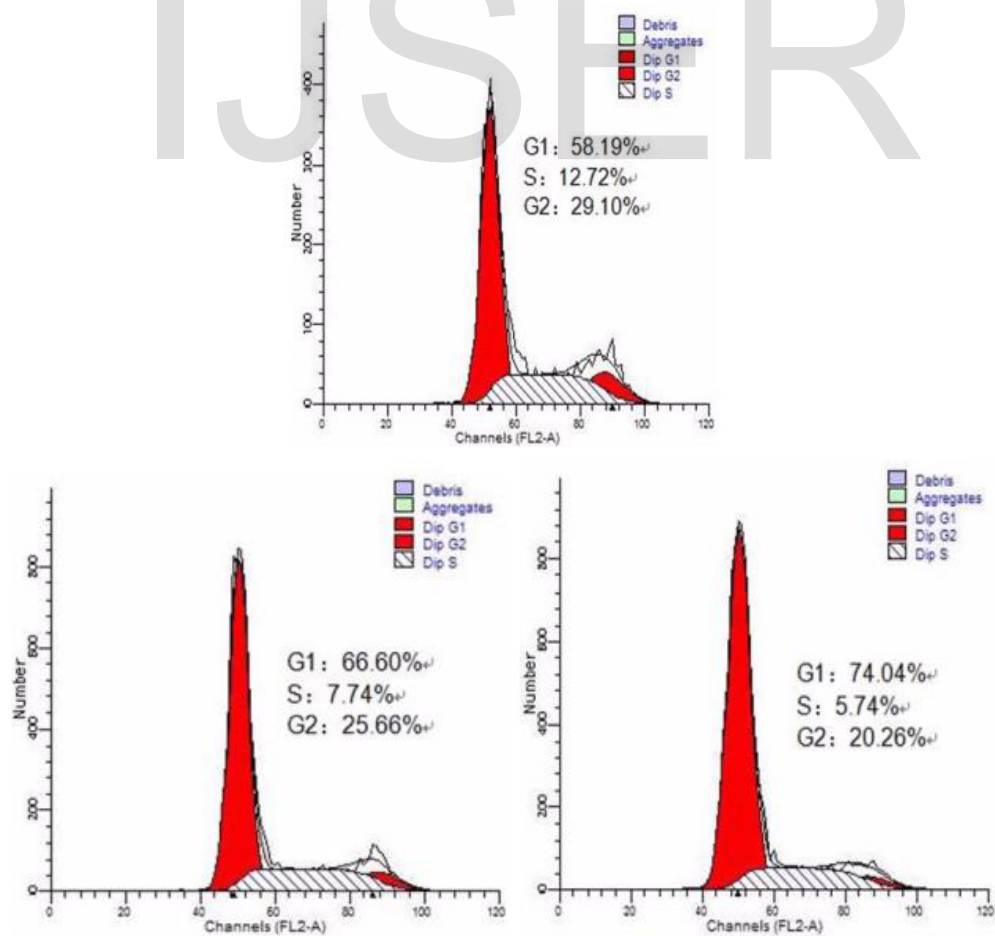
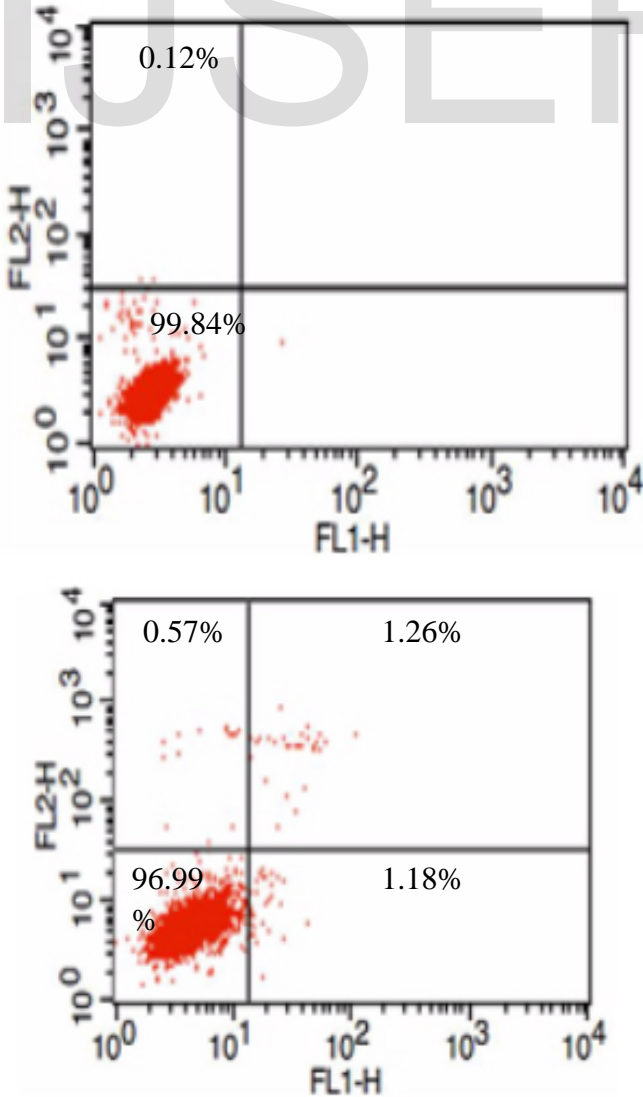


Figure 3



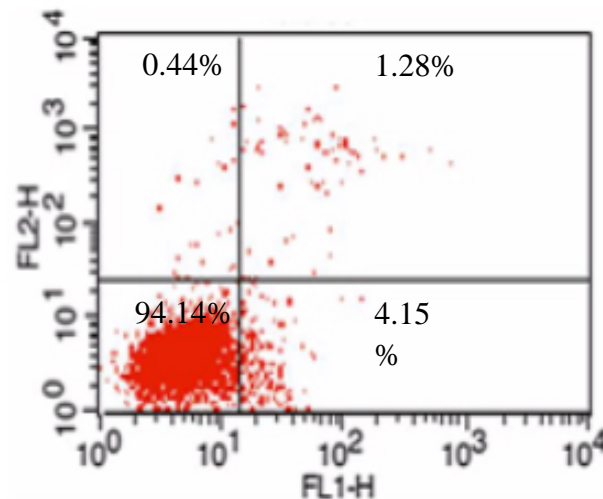


Figure 4

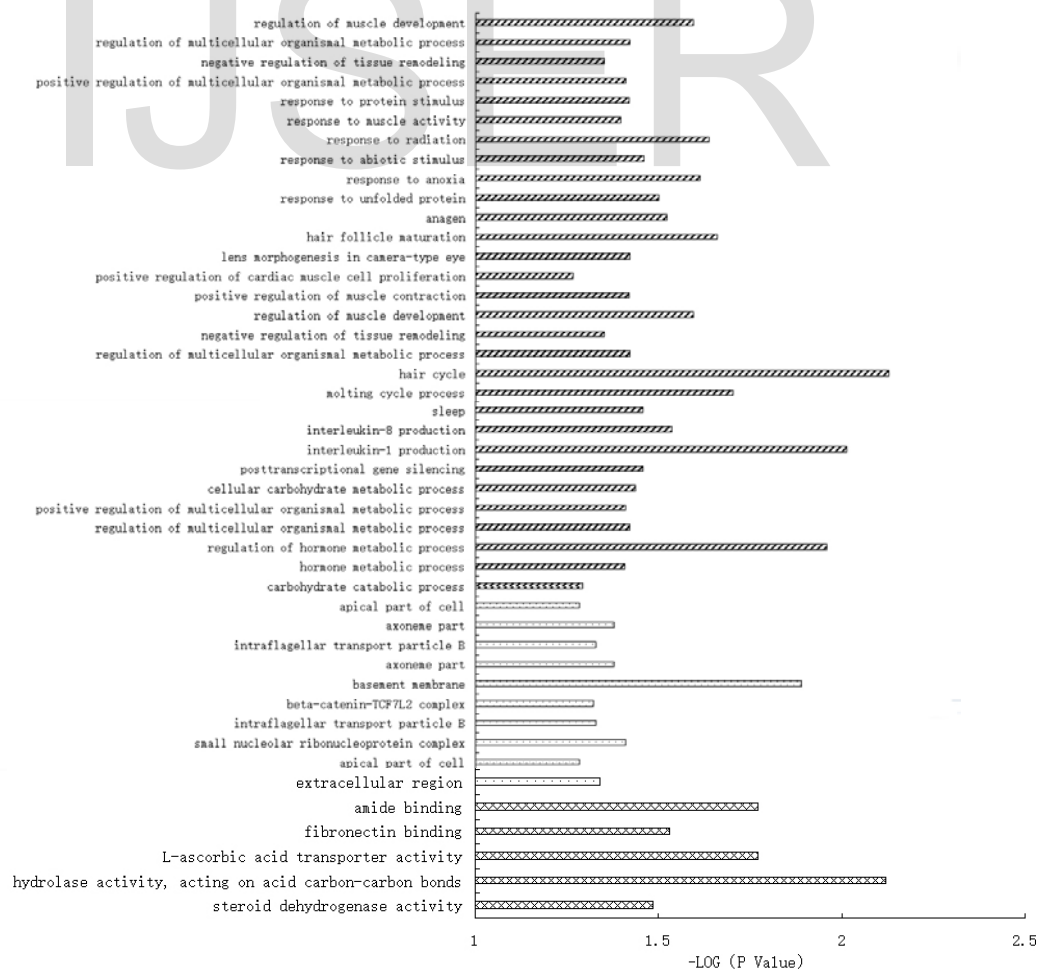


Figure 5

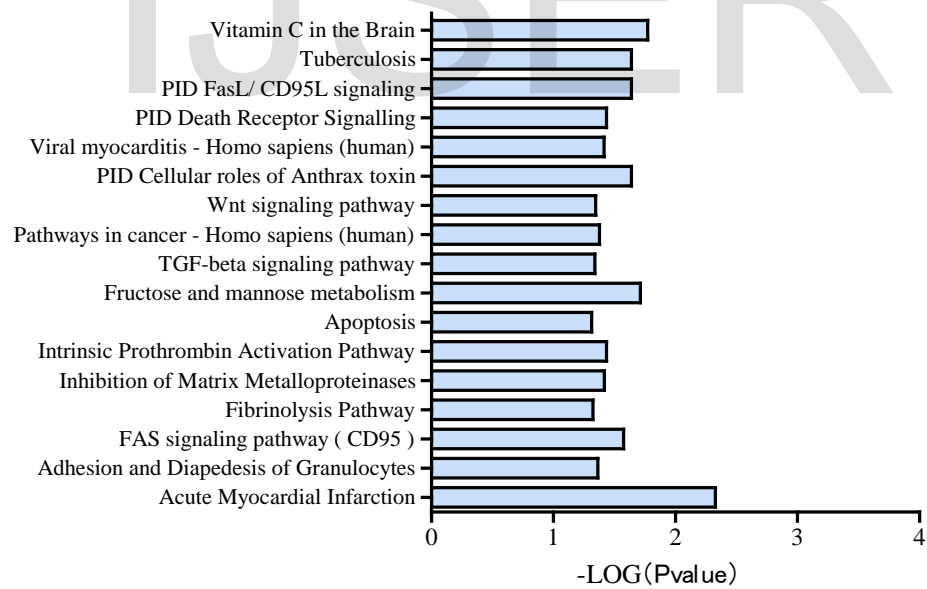
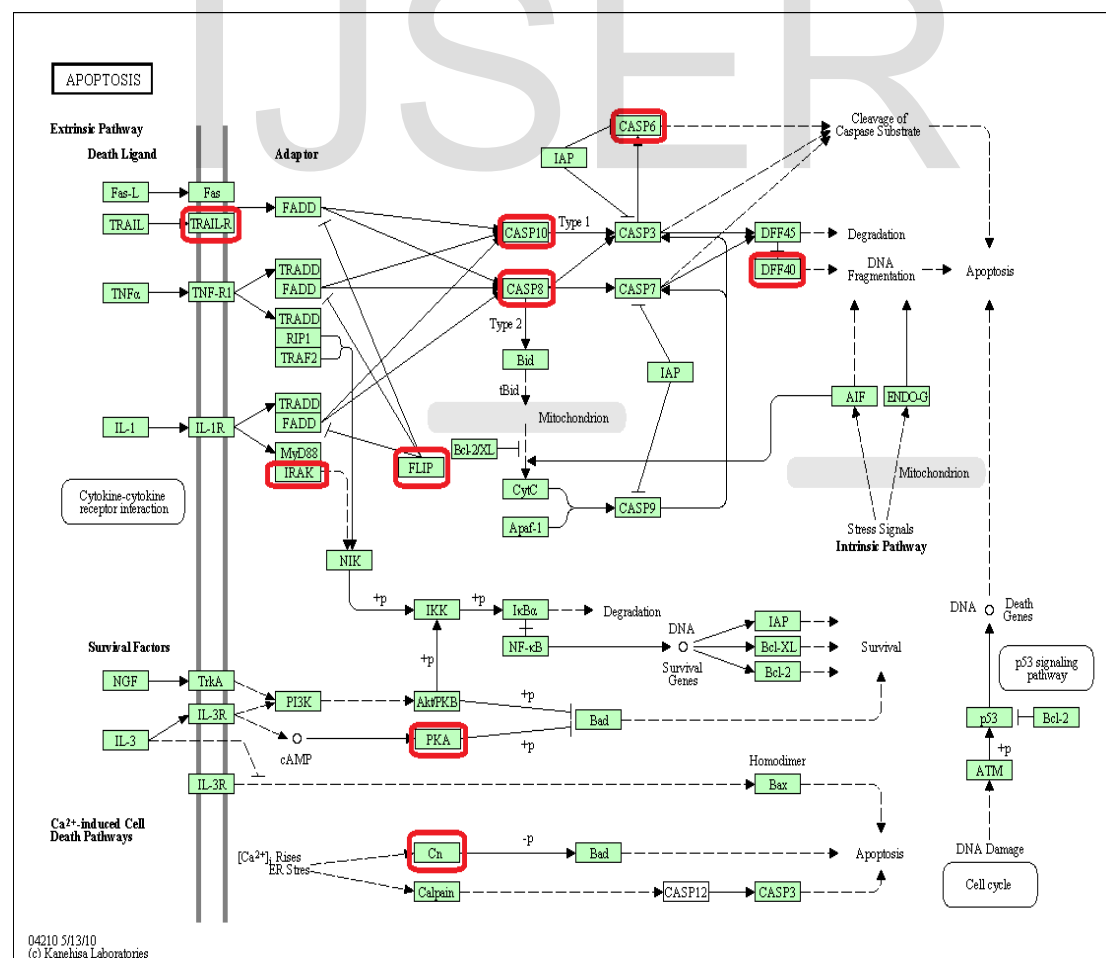


Figure 6



04210 5/13/10  
(c) Kanehisa Laboratories

Figure 7

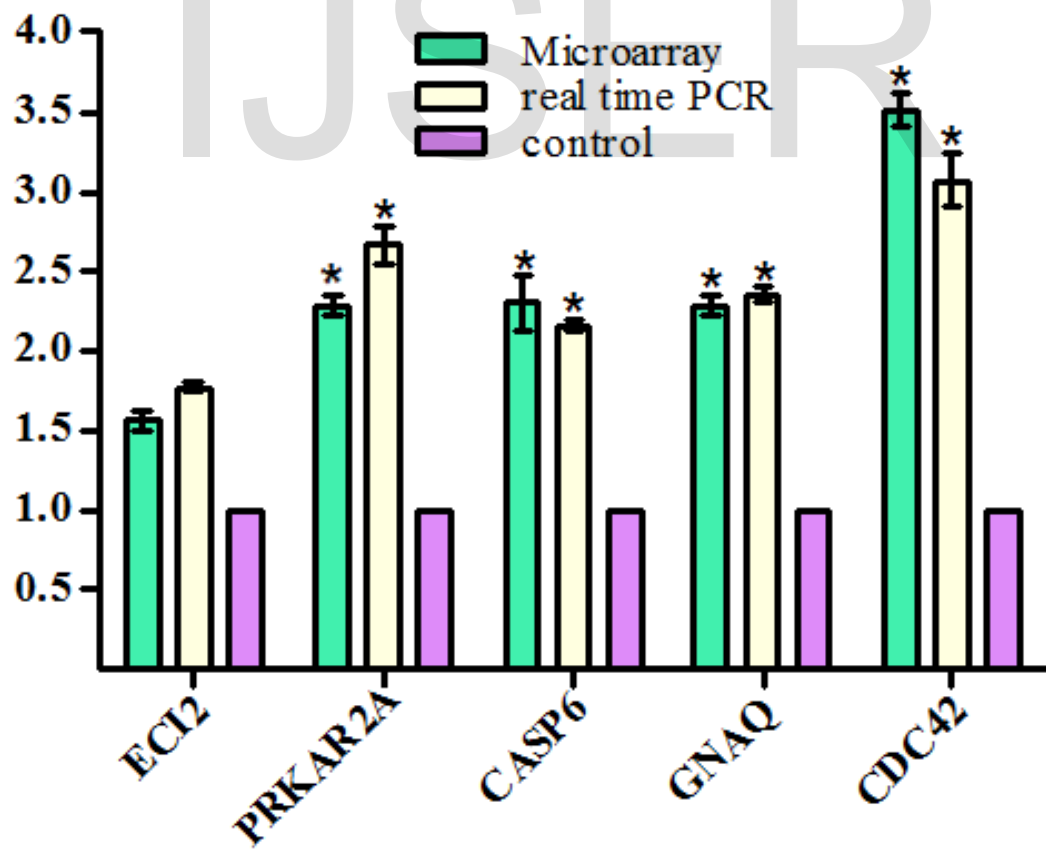


Figure 8

